Supplementary material: Design a Robot

This supplement collects derivations and extra figures that are referenced but omitted from the three-page report.

In the main report, $B(\phi)$ is obtained by intersecting the circles

$$|B - O'| = b, \qquad |B - A| = c.$$

Let $O' = (l, 0)$ and $A(\phi) = (a\cos\phi, a\sin\phi)$. Define

$$\Delta(\phi) = A(\phi) - O', \qquad r(\phi) = \|\Delta(\phi)\|.$$

Let $\hat{e}_x = \Delta/r$ be the unit vector from O' to A, and let $\hat{e}_y$ be the perpendicular unit vector (a 90° rotation). In this local basis, the circle–circle intersection point can be written as

$$B(\phi) = O' + \alpha(\phi)\,\hat{e}_x(\phi) + \beta(\phi)\,\hat{e}_y(\phi),$$

where

$$\alpha(\phi) = \frac{b^2 - c^2 + r(\phi)^2}{2r(\phi)}, \qquad \beta(\phi) = \pm\sqrt{b^2 - \alpha(\phi)^2}.$$

Geometrically, α is the signed distance from O' to the chord of intersection measured along the line of centres, and β is the signed offset perpendicular to that line. The sign choice corresponds to the two assembly modes (elbow-up / elbow-down).

A *singular (toggle) configuration* occurs when the circles become tangent, so $b^2 - \alpha^2 = 0$ and hence $\beta = 0$. Near this point the mechanism loses good transmission because the relevant links become nearly collinear [5]. See [4] for a detailed geometric derivation of the intersection construction.

S2. Feasibility over a full rotation

For real assembly, the circle intersection must exist:

$$|b - c| \le r(\phi) \le b + c.$$

In the implementation, feasibility is checked numerically by requiring $b^2 - \alpha(\phi)^2 \ge 0$ over a dense sample of $\phi \in [0, 2\pi)$. This avoids relying on case-by-case analytic inequalities when scanning many candidate designs.

A real intersection exists when

$$|b - c| \le r(\phi) \le b + c, \qquad r(\phi) = \|A(\phi) - (l, 0)\|. \tag{1}$$

At the endpoints $r(\phi) = b + c$ or $r(\phi) = |b - c|$ the circles are tangent and the mechanism is in a singular configuration (there is a unique value of B and the elbow is "straightened").

S3. Chebyshev-λ note and animation

The Chebyshev-λ mechanism is a classic four-bar family used to generate an approximate straight segment in a coupler curve, and it has been used as a simple walking mechanism [1, 3]. A short animation of one full cycle is provided with the submission as:

`chebyshev_lambda_cycle.gif`

A baseline footpath (using the default proportions from the project brief) is shown in fig. 1.

Figure 1: Baseline Chebyshev-λ geometry footpath (still image).

S4. Effect of extension length d

Keeping the four-bar fixed while increasing d amplifies the coupler curve (both stride and vertical excursion). This is why d is a high-impact design variable in the search.

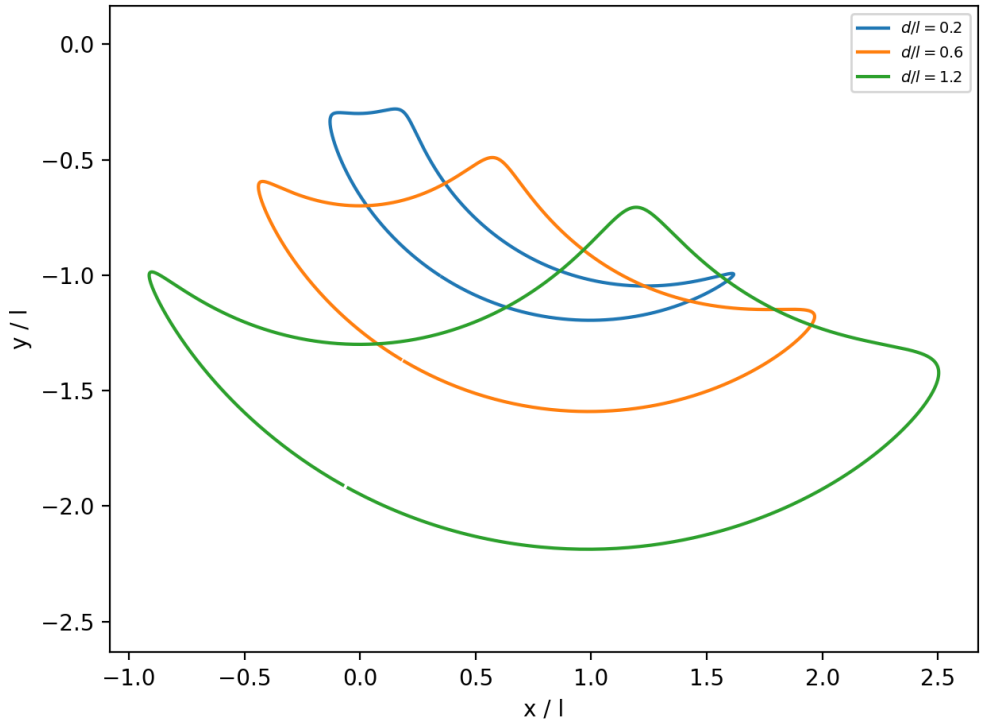

Figure 2: Effect on the foot path when varying d while keeping a, b, c fixed (example parameters as in the main draft).

S5. Transmission angle formula

For completeness, the transmission angle μ at joint B (angle between the coupler and follower) can be computed from

$$\mu(\phi) = \cos^{-1}\left(\frac{(A(\phi) - B(\phi)) \cdot (O' - B(\phi))}{\|A(\phi) - B(\phi)\| \, \|O' - B(\phi)\|}\right).$$

Very small μ corresponds to near-toggle behaviour [5].

Such is the case with design A

Figure 3 shows that Design A achieves a long, nearly horizontal stance segment, which is exactly what the geometric objective encourages. However, when we evaluate the transmission angle $\mu(\phi)$ (the angle between the coupler and the follower at joint B), the minimum value is extremely small, around 2–3°. Such a small μ indicates that the mechanism passes very close to a toggle configuration, where force transmission is poor and small actuator torques can generate large internal joint forces [3]. In practice this corresponds to high joint loads, increased strain and wear, and a greater risk of stalling or damage under real ground contact, so Design A is not a feasible choice for a physical walking robot despite the attractive trajectory.

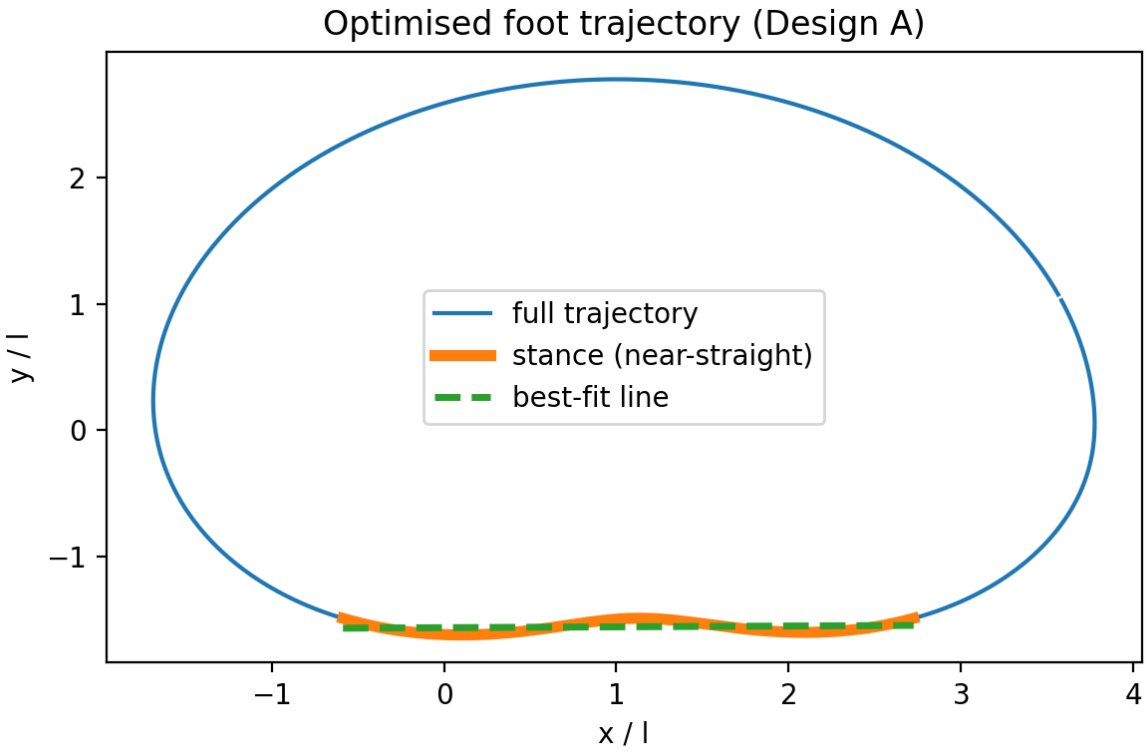

Figure 3: Foot trajectory for *Design A* (path-only optimisation). The lower segment corresponds to the stance phase extracted using the near-ground tolerance band in [2]

1 Design A: geometric optimisation

A random search over $(\bar{a}, \bar{b}, \bar{c}, \bar{d})$ was performed, rejecting samples that violate feasibility for a full input rotation. The best geometric design found (denoted *Design A*) was

$$\boxed{\frac{a}{l} = 1.13, \qquad \frac{b}{l} = 1.32, \qquad \frac{c}{l} = 1.20, \qquad \frac{d}{l} = 1.46.} \tag{2}$$

Its foot trajectory is shown in fig. 3, and two representative linkage configurations are shown in the the main project discussion.

For the stance segment in fig. 3, the measured values are approximately

$$\Delta x \approx 3.31\, l, \qquad E \approx 0.078\, l, \qquad \text{duty factor} \approx 0.50.$$

For *Design A*, fig. 3 shows that μ becomes very small (about 2.3°), which explains why a purely path-based optimisation can hide a mechanically undesirable configuration.

2 Four-leg knee (B) trajectories and centre-of-mass motion

To illustrate how the single-leg module behaves when combined into a simple quadruped, we implemented a basic four-leg kinematic simulation in Python. Each leg uses the same linkage geometry and is assigned a fixed phase offset (walk sequence) so that legs alternate between stance and swing. During stance, the corresponding foot point is treated as approximately fixed on the ground, and the body position is adjusted to satisfy the stance constraint.

For visualisation, we plot the world-frame trajectory of the knee joint B for all four legs together with the mass-weighted centre-of-mass (COM) path of the robot (including the body mass and uniform rod masses for the links). The COM exhibits a periodic "bobbing" motion over the gait cycle, reflecting the alternating support pattern and changing configuration of the leg link masses.

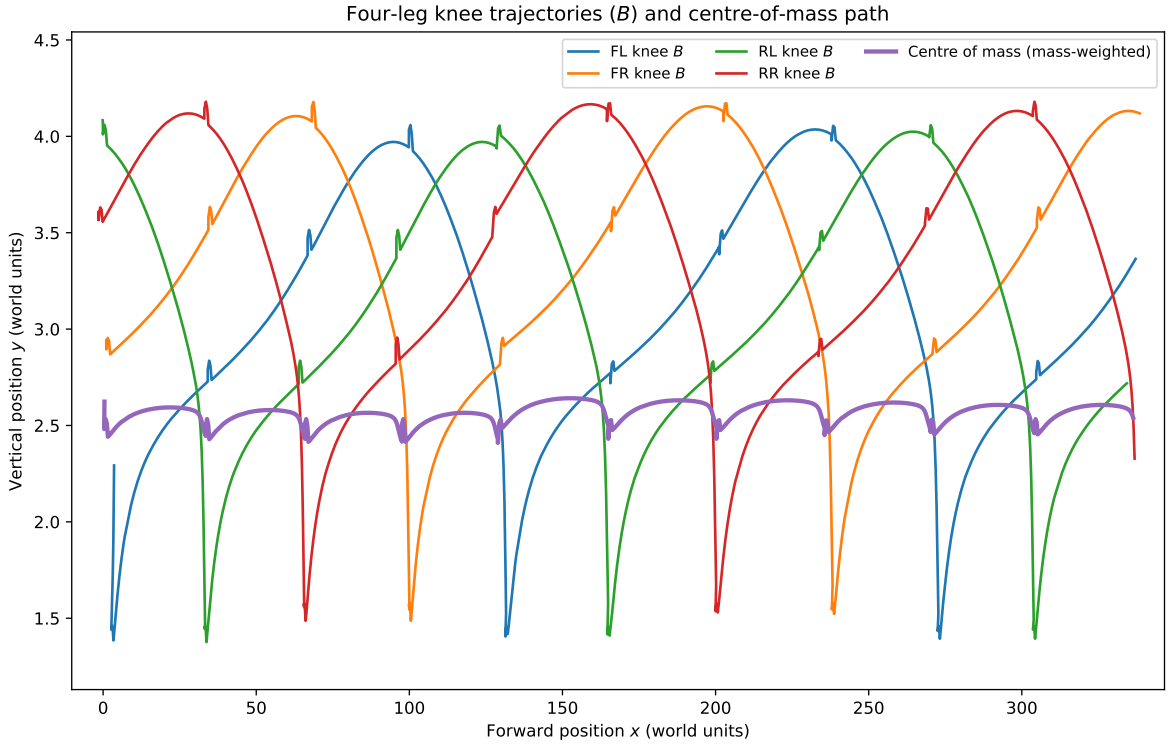

Figure 4: Four-leg simulation results: knee-joint trajectories (joint B) for each leg (FL, FR, RL, RR) and the mass-weighted centre-of-mass (COM) path over multiple gait cycles. The COM shows periodic vertical oscillation ("bobbing") as the support pattern alternates between stance and swing phases.

References

[1] D. Miler, D. Birt, and M. Hoić, "Multi-Objective Optimization of the Chebyshev Lambda Mechanism," *Strojniški vestnik – Journal of Mechanical Engineering*, vol. 68, no. 12, pp. 725–734, 2022.

[2] E. Connaghan, *AMA3020: Design a Robot (code and figures)*, GitHub repository, 2026. `https://github.com/eoghanedwardconnaghan-bot/AMA3020-Design-A-Robot`

[3] A. Baskar, M. Plecnik, and J. Hauenstein, "Finding Straight Line Generators through the Approximate Synthesis of Symmetric Four-bar Coupler Curves," 2022.

[4] H. H. Asada, *Introduction to Robotics: Chapter 4 — Planar Kinematics*, MIT OpenCourseWare / course notes.

[5] J. Angeles and S. Bai, *Lecture Notes on Kinematic Synthesis*, McGill University, January 2016.